Electronic supplementary information (ESI)

Weaving electron-rich Alkynes: a durable *in situ* skin for stabilizing zinc anodes

Xin Liu,‡[abe] Weimian Zhang,‡[b] Ying Liu,‡[a] Xiaodong Li,[a] Deyi Zhang,[ac] Kun Wang,[d] Lifeng Liu,[b] Changshui Huang*[ace]

[a] Beijing National Laboratory for Molecular Sciences, Organic Solids Laboratory, Institute of Chemistry, Chinese Academy of Science, Beijing 100190, China, E-mail: huangcs@iccas.ac.cn

[b] Songshan Lake Materials Laboratory (SLAB), Dongguan 523808, China

[c] University of Chinese Academy of Sciences, Beijing 100049, China

[d] Qingdao Xintaihe Nano Technology Co., Ltd, Qingdao 266600, China

[e] Qingdao Institute of Bioenergy and Bioprocess Technology, Chinese Academy of Sciences, Qingdao 266101, China

1. Preparation of e-TDYP@Zn.

Fig. S1 shows the schematical illustration of synthesis process of tetraethynylthiophene (TET) monomer and e-TDYP@Zn. 2g (5mmol) of 2, 3, 4, 5−tetrabromothiophene, 6.2 ml (45mmol) of $(CH_3)_3SiC{\equiv}CH$, 0.351 g (0.500 mmol) of $PdCl_2(PPh_3)_2$, 0.152 g (0.8 mmol) of CuI, and 0.2096 g (0.8 mmol) of were added into mixture of 80 mL TEA. The mixture was stirred under an argon atmosphere at 60 ℃ for 3 days in a tube sealing. The solvent was evaporated and the residue was then purified by columnchromatography to yield tetra(trimethylsilyl)ethynylthiophene as pale-yellow powder (1.85 g). To a solution of 43.2 mg (0.1 mmol) tetra (trimethylsilyl)ethynylthiophene in 15 mL THF was added 0.4 mL TBAF (1M in THF, 0.4 mmol) and stirred at 0 °C for 30 min. The solution was then diluted with CH_2Cl_2 and washed with distilled water and dried with anhydrous Na_2SO_4. The solvent was removed in vacuum rotary evaporation to yield TET.

The e-TDYP with assigned morphology on zinc substrate was synthesized using a modified Glaser–Hay coupling reaction. The zinc plates (2×5 cm, 10 pieces) and copper plate (4×12 cm, 10 pieces) were carried out an ultrasonic cleaning in 0.1 M hydrochloric acid for 30 seconds. The materials were then cleaned with deionized water, ethanol, and acetone solvent for 10 minutes each in the ultrasonic cleaner, and then dried in argon atmosphere. Prior to dripping 20 mL of pyridine containing 50 mg of TET monomer to the reaction unit, the folded copper-zinc envelopes were placed in a three-necked flask with 80mL mixed solvent of acetone, anhydrous pyridine, and TMEDA with volume ratio of 100:5:1 under argon atmosphere. The pyridine dripping process was proceeded at an even speed for 2 h by an argon-protected constant pressure funnel. After keeping the system at 50°C for 12 h, zinc plates were uncovered and washed with ethanol and acetone several times in turn and dried at 100 °C under vacuum to obtain the e-TDYP@Zn.

2. Material Characterizations

The morphology of e-TDYP@Zn was characterized by scanning electron microscopy (SEM, HITACHI S-4800) and transmission electron microscopy (TEM, JEM2100PLUS). The X-ray diffraction (XRD) of e-TDYP@Zn and Zn foil were obtained by diffractometer (Bruker D8 ADVANCE) under Cu Kα irradiation at λ = 1.5406 Å. The Raman spectra of e-TDYP@Zn and Zn

excited by the Ar laser of 532 nm were recorded at room temperature using a DRXXI system from Thermo Scientific. Fourier transform infrared spectrometer (FT-IR, Thermo Fisher Scientific Inc. Nicolet iN10) were employed to analyze the surface properties of the electrode. X-ray photoelectron spectroscopy (XPS, VG Scientific ESCA Lab220i-XL) was performed to detect the surface compositions of electrodes after soaking in 2 M ZnSO4 with Al Ka radiation as the excitation source. The obtained spectra were analyzed using XPS peak software.

The time-of-flight secondary-ion mass spectrometry (TOF-SIMS) measurements were performed using a PHI nano TOF II (ULVAC-PHI, Japan). A Bi_3^{++} liquid metal ion gun (LMIG) with an energy of 30 keV was used as the primary ion source to analyze a surface area of 80 μm × 80 μm. For depth profiling, an argon gas gun (Ar^+) was employed as the sputter ion source, operating at 4 kV with a current of 200 nA, covering a sputter area of 400 μm × 400 μm. The relative sputtering rate was calibrated against SiO_2 and found to be approximately 0.83 nm/s under the given conditions. The e-TDYP sample was analyzed after 20 cycles of galvanostatic plating/stripping in symmetric cells at current density/areal capacity of 1 mA cm^{-2}/1 mAh cm^{-2}.

3. Electrochemical Measurements.

The CR2032 coin cells were assembled in air and subjected to symmetric cell, asymmetric cell, and full cell tests. Electrodes of bare Zn, e-TDYP@Zn and copper foil were cut into circles with a diameter of 12 mm and a glass fiber filter with diameter of 16 mm was used as a separator (Whatman). The symmetrical cell is assembled from two identical zinc electrodes. The asymmetric cell was carried out using the copper foil as the working electrode and the zinc plate as the counter electrode. The full cell is coupled with MnO_2 and I_2 cathode. MnO_2 electrodes were prepared by applying a slurry to carbon paper (Toray Industries, Inc.) before drying in a vacuum oven at 60 °C for 12 h. The slurry consisted of lab-made MnO_2, carbon nanotube and PVDF in a mass ratio of 7:2:1. The lab-made α-MnO_2 nanorods were prepared by a hydrothermal method through potassium permanganate ($KMnO_4$) following the reported procedure. The mass loading of MnO_2 was around 1-2 mg cm^{-2} and the thickness of zinc foil is 50 μm for regular tests. The mass loading of MnO_2 was around 8 mg cm^{-2} and the thickness of Zn foil was 10 μm for N/P = 2.7 tests. The mass loading of MnO_2 was around 8 mg cm^{-2} and the thickness of Zn foil was 10 μm for N/P = 2.7 tests. The thickness of zinc foil for

symmetrical cell performance test with high DOD is 20 or 30 μm. The electrochemical measurements of half cells are performed in 2 M $ZnSO_4$ solution. Zn||MnO_2 full cell performance were performed for adding extra 0.2 M $MnSO_4$ in 2 M $ZnSO_4$.

Cell performance tests were characterized by LAND electrochemical station for cycling stability. Other electrochemical performances such as Cyclic Voltammetry (CV), Electrochemical Impedance Spectroscopy (EIS), Tafel curves, chronoamperometry (CA) and LSV curves were measured by a CHI660E electrochemistry workstation. The Zn plating/stripping performance was measured in Zn||Zn symmetrical cells. The shelving-recovery tests of symmetrical cells of e-TDYP are operated at current density/areal capacity of 5 mA cm^{-2} / 5 mAh cm^{-2}, subsequently applied with an alternating shelving period of 50 hours after 25 × N cycles (N = 1, 2, 3 ……).

The exchange current density was calculated by linear fitting the relationship between the overpotential and current density based on Fig. 2b using the Butler-Volmer approximation equation to evaluate the kinetics of deposition:

$$i = i_0 \frac{F}{RT} \cdot \frac{\eta}{2}$$

where F is the Faraday's constant, R is the ideal gas constant, T is the Kelvin temperature, and η is the overpotential of reduction. The CE of Zn anodes was measured with Zn||Cu cells at a current density of 2 mA cm^{-2} and 4 mA cm^{-2}. The electrochemical performance of Zn||MnO_2 full cell was tested in a voltage range of 0.8-1.8 V.

The electrochemical stability of the e-TDYP@Zn for anticorrosion is tested via a three-electrode system in 2 M ZnSO4 electrolyte for comparing with bare Zn. The electrochemical stability of the electrodes was evaluated using linear sweep voltammetry (LSV) at a scan rate of 10 mV s^{-1} with stainless steel (SS) electrodes. The electrochemical impedance spectroscopy (EIS) of the full cells in the frequency range of 0.01-100 kHz and CV curves at a scan rate of 0.5 mV s^{-1}. The amount of electrolyte for single coin cell was ≈100 μL. The DEMS test was carried out by measuring the

hydrogen evolution of symmetric cell at 0.05 mA / 0.5 mAh using a commercial system (Hiden HPR-40) with an ECC-DEMS cell.

4. Finite element analysis.

Finite element analysis (FEA) was employed in this study to simulate the behavior of the e-TDYP@Zn anode interface under electrochemical cycling. COMSOL Multiphysics was used to construct a 2D model of the electrolyte and electrode interface environment with a size of 3×6 μm. Semicircles were utilized to represent the surface protuberances on the Zn electrode, while the in situ synthesized e-TDYP was modeled by a space with a width of 200 nm between two rectangles with a size of 0.02×1 μm. Porous electrodes were used to describe the three-dimensional structure e-TDYP with permeability to electrolyte and electrical conductivity through its domains. The simulation uses continuity equation to calculate the material balance in the electrolyte, and Nernst-Planck equation to the flux. Electrode reaction kinetics are given by the Butler-Volmer equation. The model of e-TDYP is built as multiple uniformly distributed porous regions with negative charges grown on the anode due to its electronegative nature. The simulated model does not consider possible side reactions. The vertical walls and the bottom edges of the GDY are assumed to be insulation boundaries. Post-processing is conducted to investigate the distribution of current density and Zn^{2+} ionic concentration.

5. Theoretical Calculations.

Density functional theory (DFT) calculations were carried out using Gaussian 16 packages. Models for all computational molecules were optimized by B3LYP functional with a 6−31+G (d,p) basis set and D3 dispersion correction. Frequency calculations using M06-2x functional were performed to determine the nature of a stationary point as the true local minimum. The electrostatic potential (ESP) mapping was postprocessed with Multiwfn 3.9 and Visual Molecule Dynamics (VMD).

The adsorption energies E_{ads} were defined as:

$$E_{ads} = E_{total} - E_{sub} - E_{Zn^{2+}}$$

where E_{total} is the total energy of the system, E_{sub} is the energy of the e-TDYP model, $E_{Zn^{2+}}$ is the energy of Zn^{2+}.

The desolvation energy E_{de} was calculated by the following equation:

$$E_{de} = E_{Zn(H_2O)_6{}^{2+}} - E_{Zn(H_2O)_5{}^{2+}} - E_{H_2O}$$

where $E_{Zn(H_2O)_6{}^{2+}}$, $E_{Zn(H_2O)_5{}^{2+}}$, and E_{H_2O} are the energy of $Zn(H_2O)_6{}^{2+}$, $Zn(H_2O)_5{}^{2+}$ and H_2O respectively.

The adsorption energy of H atom $E_{ads(H)}$ was calculated by the following equation:

$$E_{ads(H)} = E_{H@cat} - E_{cat} - E_H$$

where the $E_{H@cat}$ is the total energies of catalyst surface with adsorbed H species, E_{cat} represents the energy of catalyst surface, E_H is one-half the energy of gas-phase H_2.

The hydrogen adsorption free energy is derived from

$$\Delta_G = E_{ads(H)} + \Delta E_{ZPE} - T\Delta S$$

where ΔE_{ZPE} and ΔS are the changes in zero-point energy and entropy, respectively.

At T=298.15 K, ΔG can be obtained by $\Delta G = E_{ads(H)} + 0.24$ eV.

6. Figures S1-S20

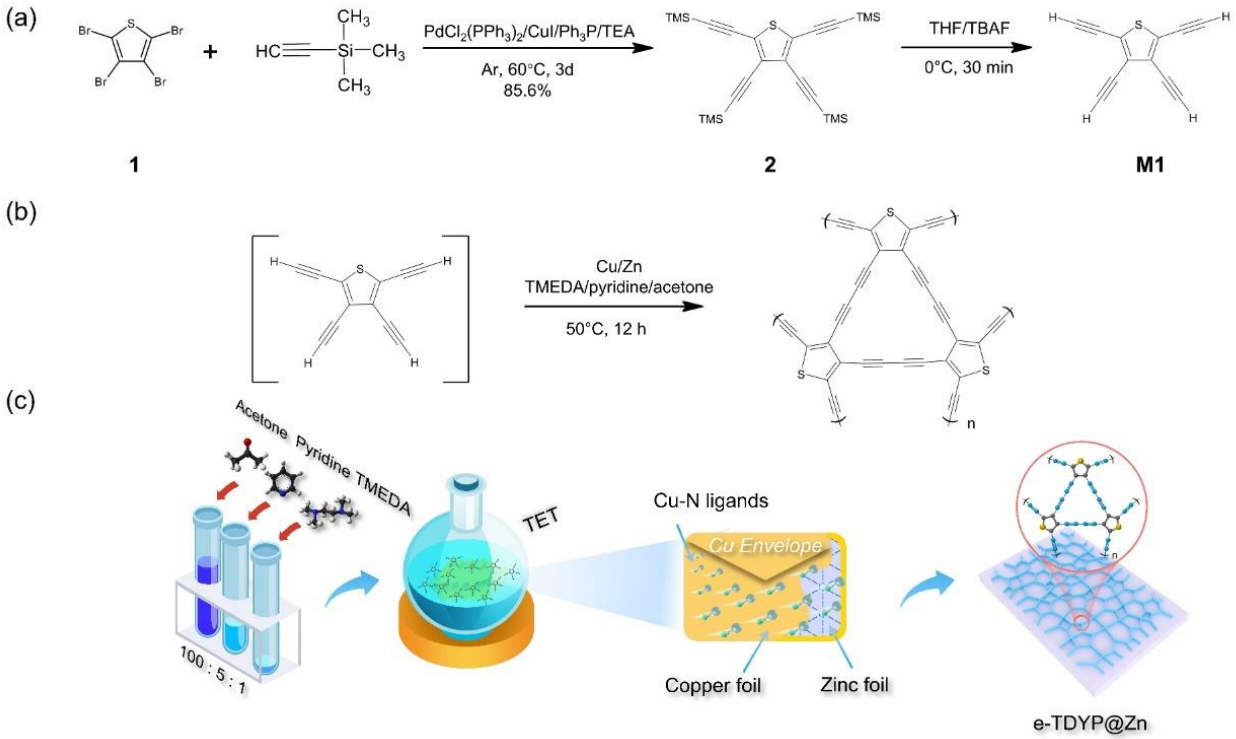

Fig. S1 (a) Synthesis of 2,3,4,5-tetrakis[(trimethylsilyl)ethynyl]-thiophene (2) and 2,3,4,5-tetraethynylthiophene (M1). (b) Synthesis of thiophdiyne. (c) Schematical illustration of formation mechanism of e-TDYP@Zn.

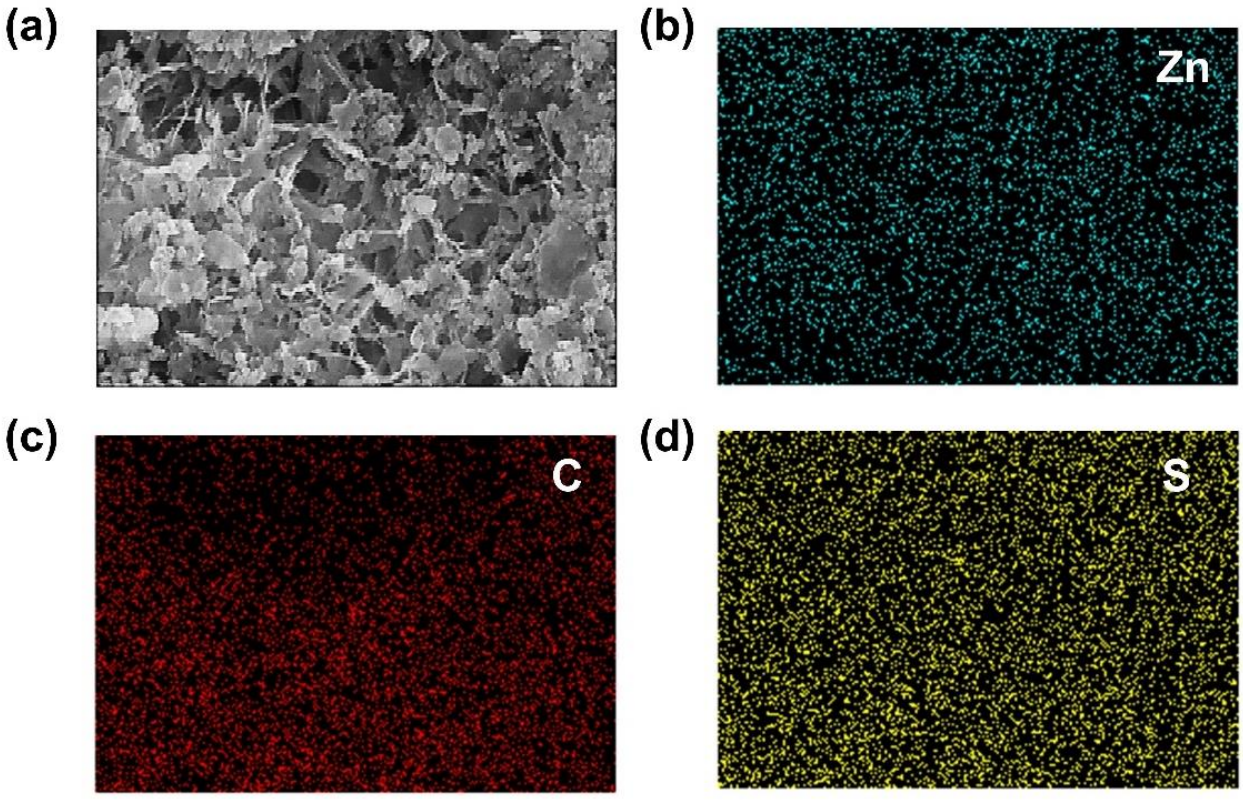

Fig. S2 (a) Top-view SEM image of e-TDYP@Zn and (b-d) the corresponding elemental dispersive X-ray spectroscopy (EDS) mappings.

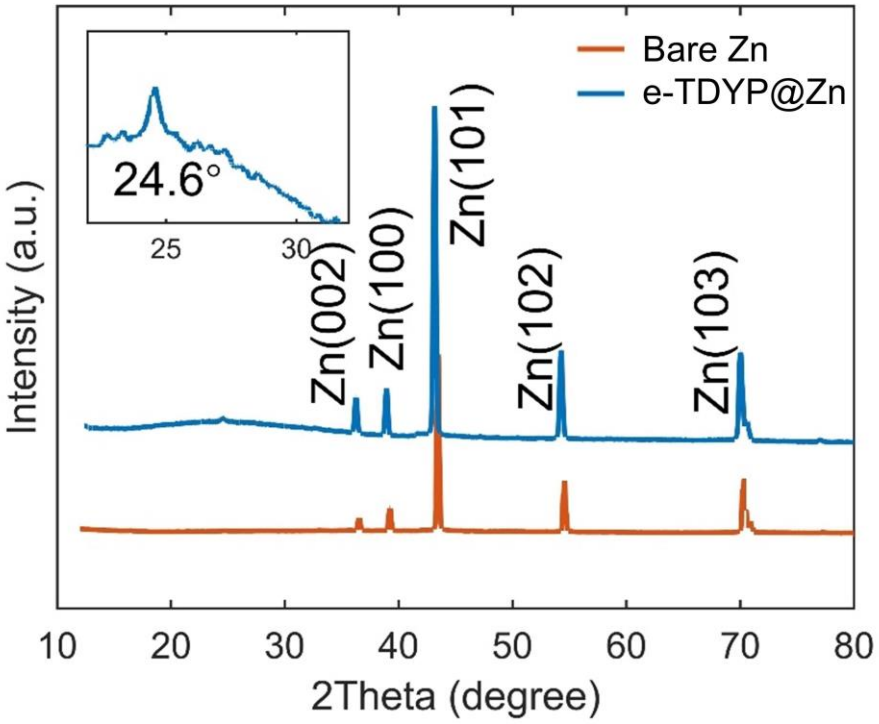

Fig. S3 Comparison of the XRD patterns of e-TDYP@Zn and bare Zn.

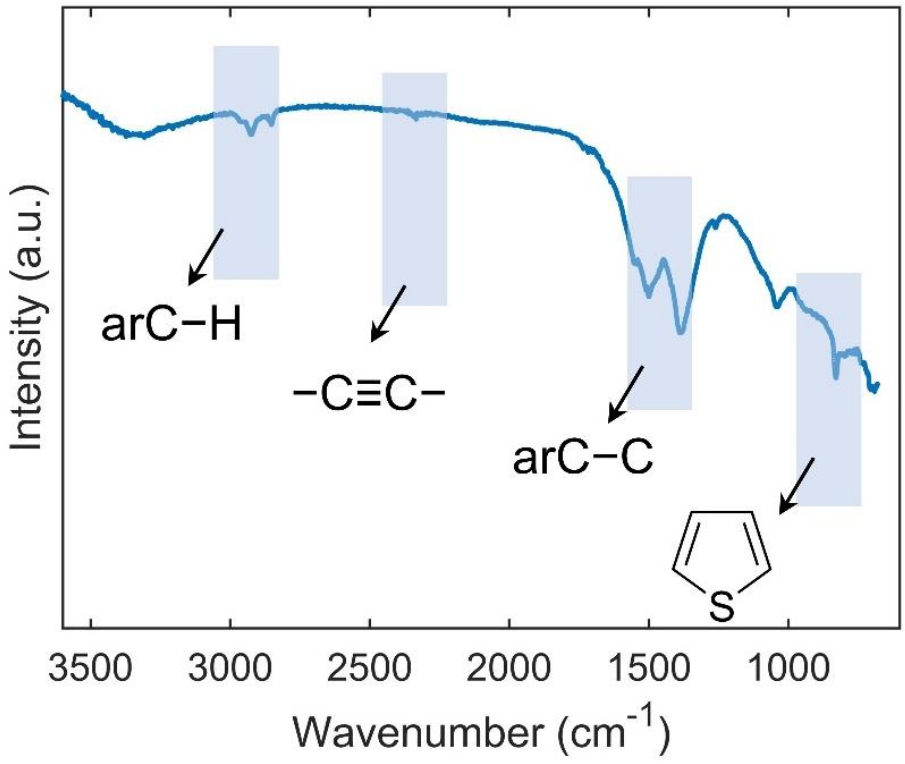

Fig. S4 FTIR spectra of the e-TDYP@Zn

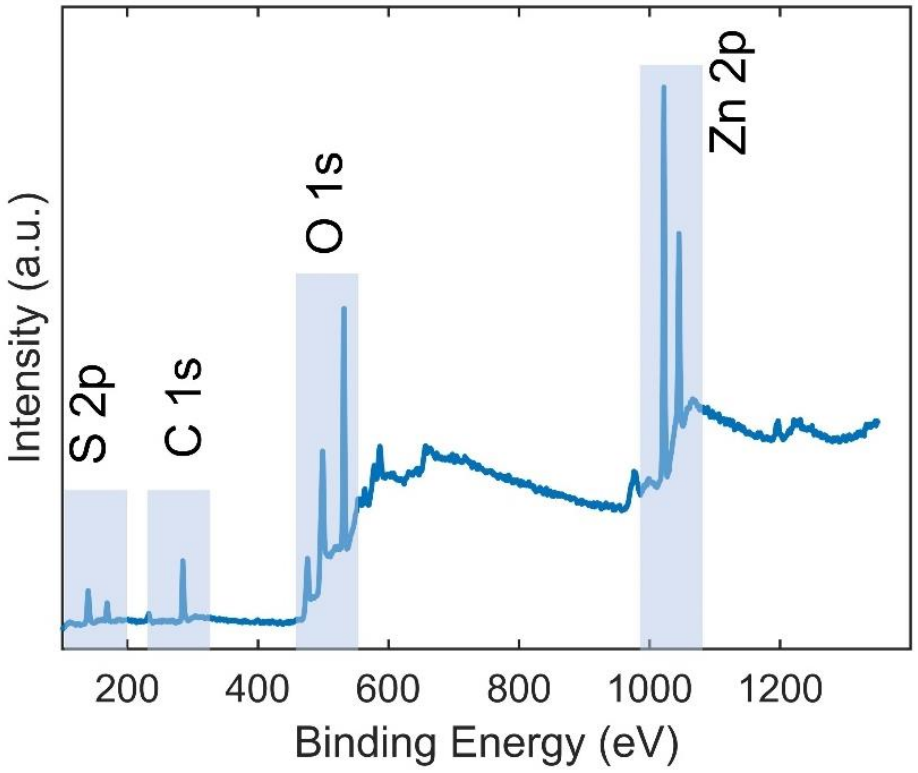

Fig. S5 Full XPS spectrum of e-TDYP@Zn.

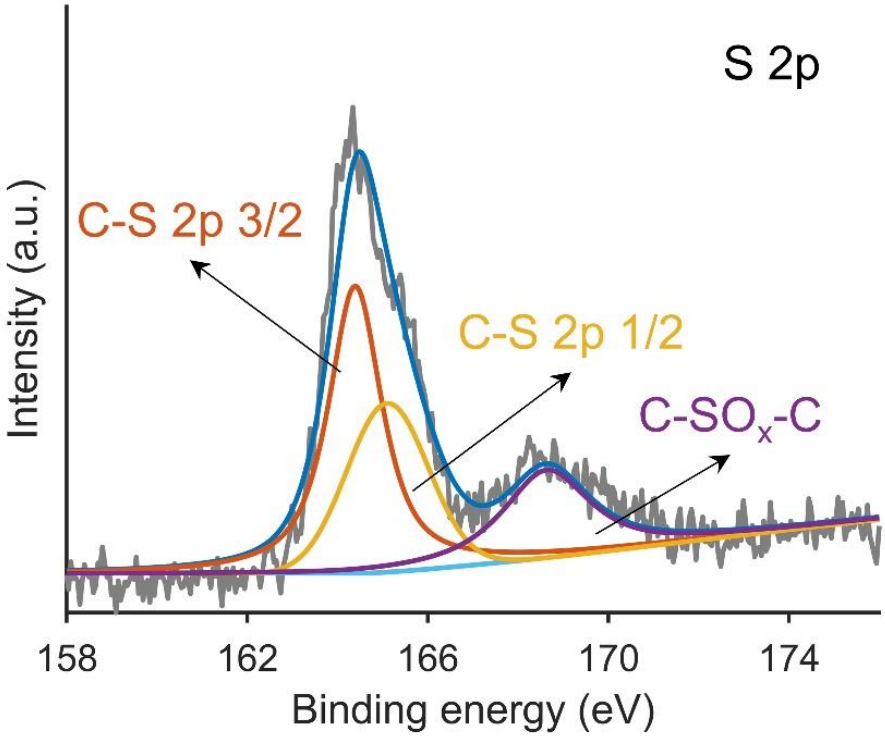

Fig. S6 S 2p XPS spectra of e-TDYP@Zn.

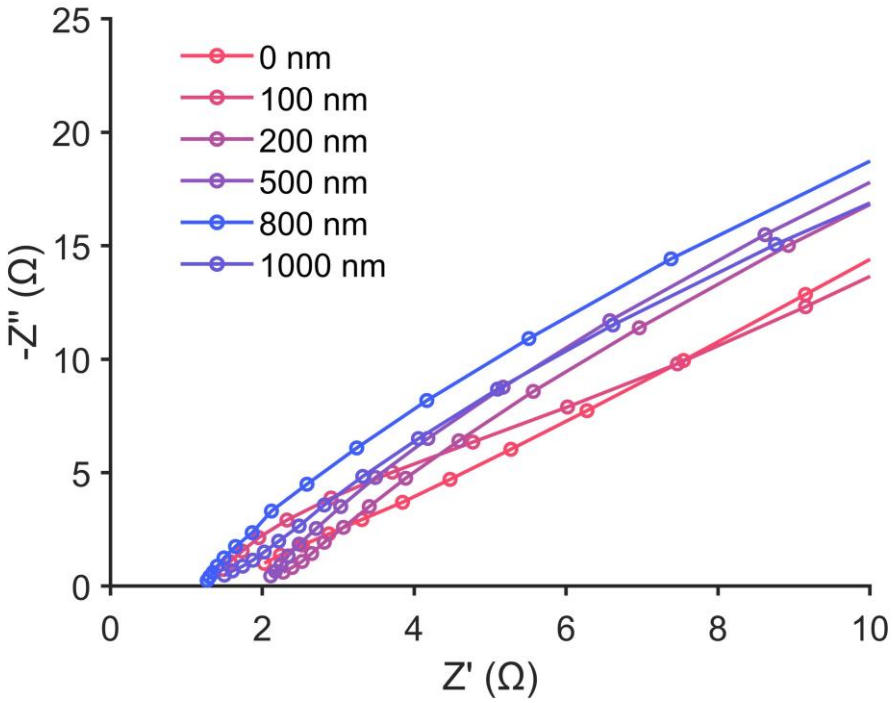

Fig. S7 The Nyquist plots for symmetric cells with different thickness of e-TDYP.

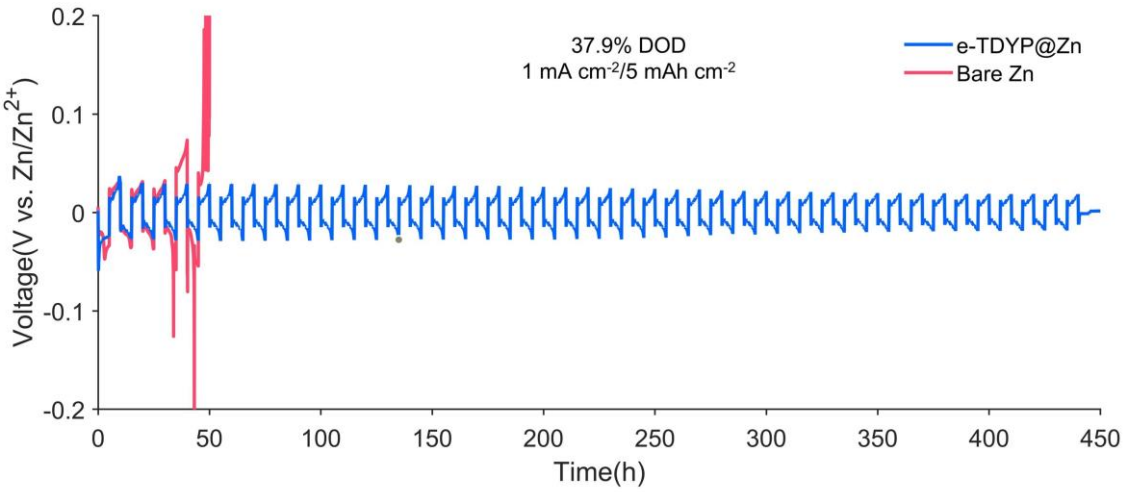

Fig. S8 Voltage profiles of symmetric cells with e-TDYP@Zn and bare Zn anodes at current density/areal capacity of 1 mA cm^{-2}/5 mAh cm^{-2}.

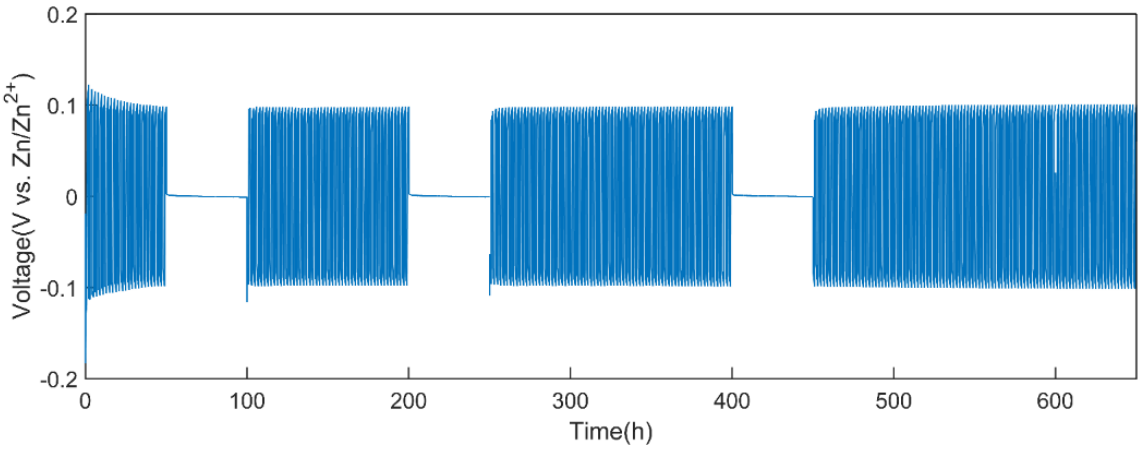

Fig. S9 The shelving-recovery performances for e-TDYP@Zn under 5 mA cm^{-2} and 5 mA h cm^{-2}.

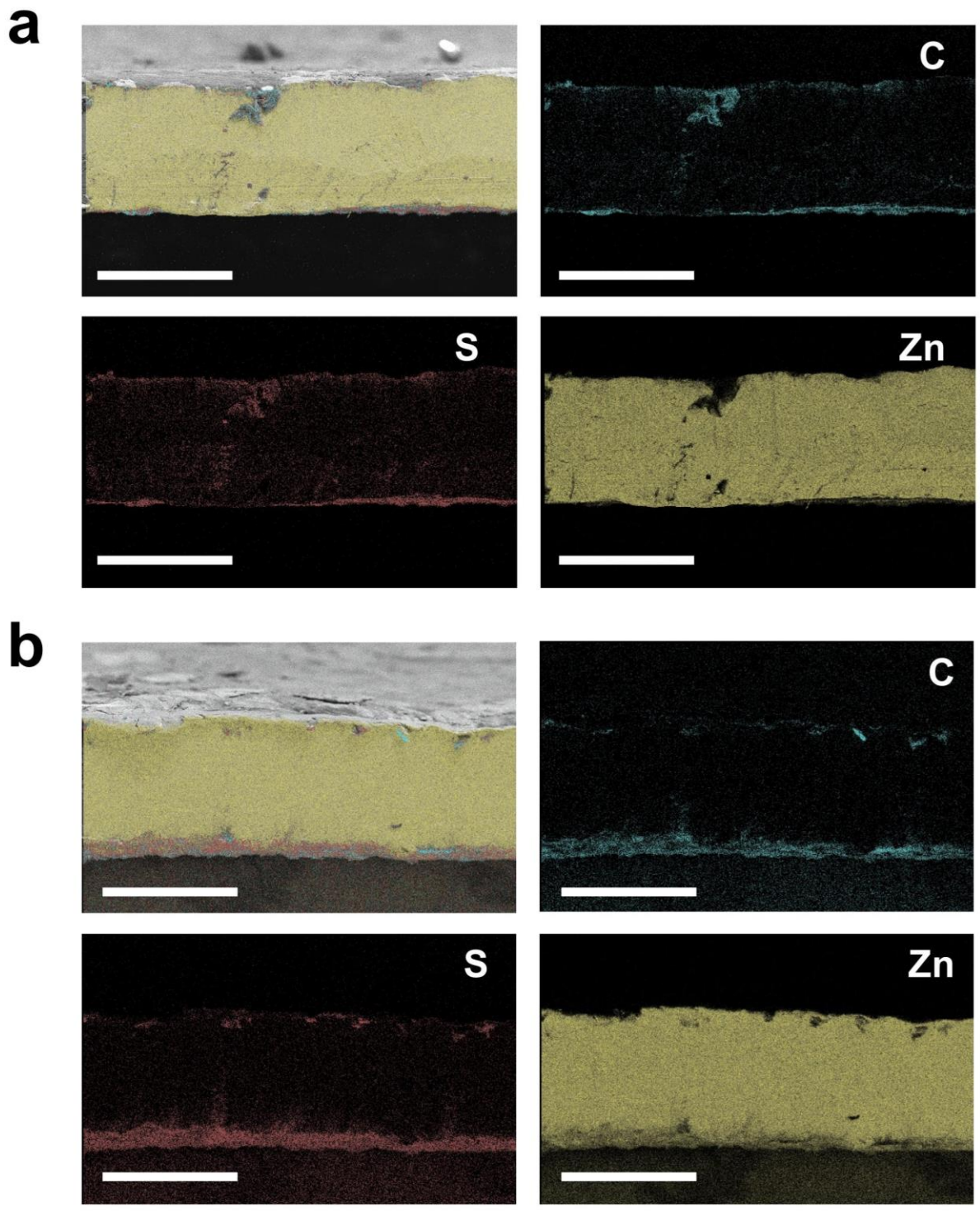

Fig. S10 Cross-sectional SEM images of e-TDYP@Zn: (a) before and (b) after deposition at a current density of 1 mA cm^{-2} for 1 hour. The scale bars for SEM images are all equivalent to 100 μm.

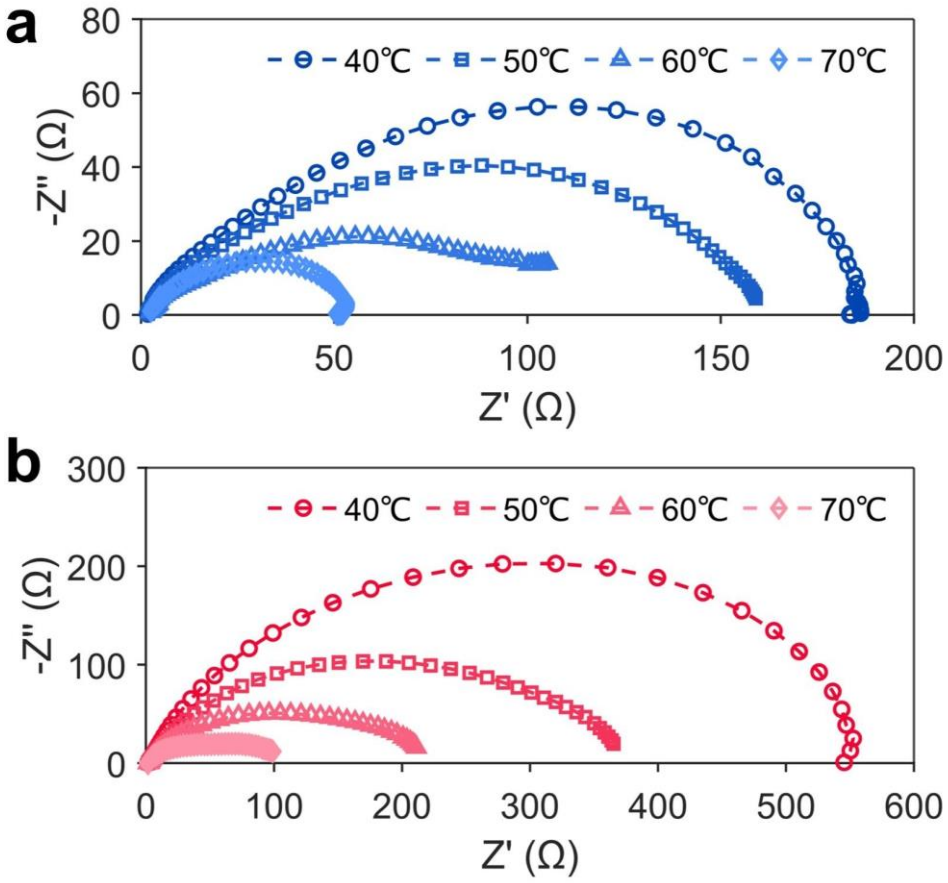

Fig. S11 The EIS plots of (a) e-TDYP@Zn electrode and (b) bare Zn electrode at different temperatures.

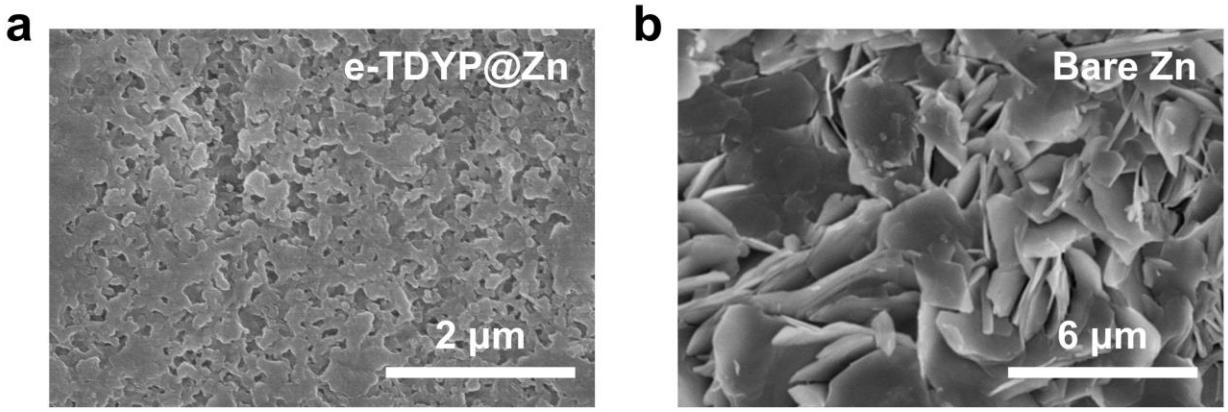

Fig. S12 SEM images of (a) e-TDYP@Zn and (b) bare Zn anodes after cycling.

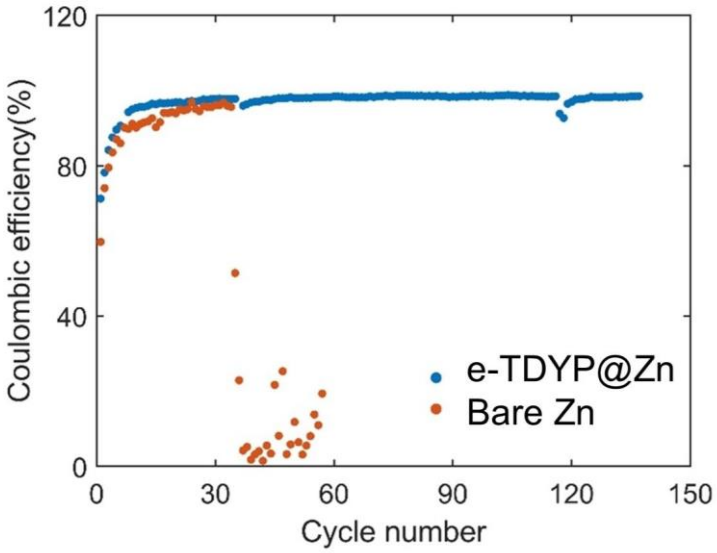

Fig. S13 Coulombic efficiency of Zn plating/stripping 1 mAh cm^{-2} at current densities of 2 mA cm^{-2}.

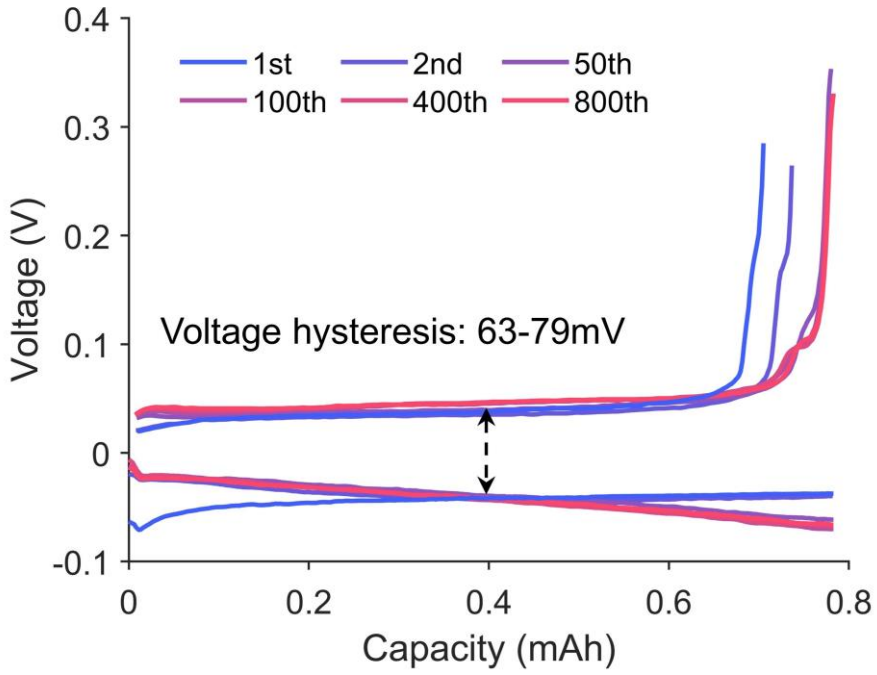

Fig. S14 Voltage hysteresis of e-TDYP@Zn anode at 4 mA cm^{-2} for 1 mAh cm^{-2}.

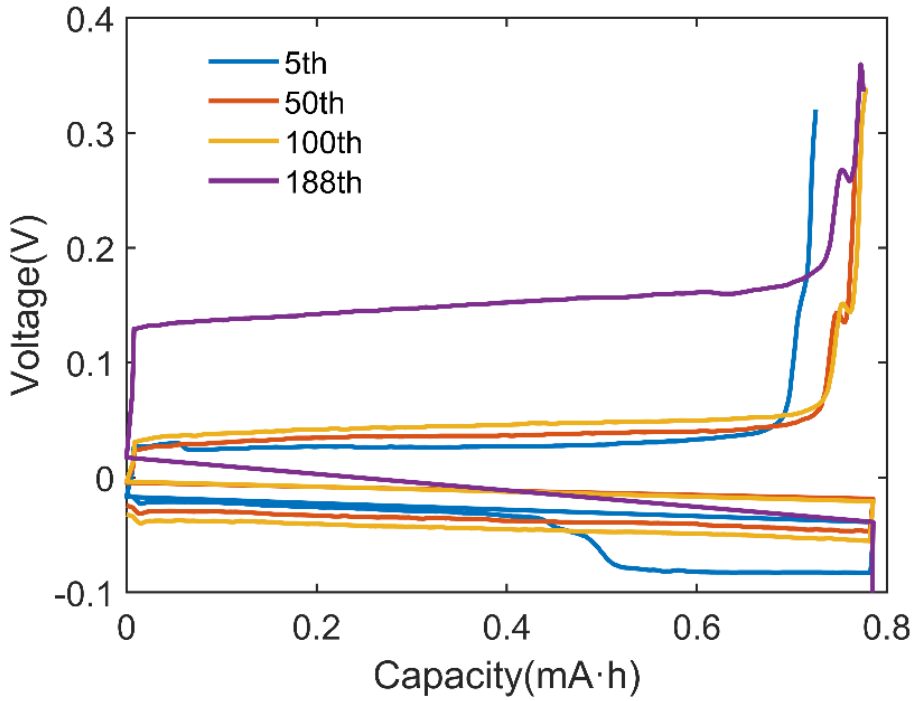

Fig. S15 Voltage profiles of Cu||bare Zn at 4 mA cm^{-2} for 1 mAh cm^{-2}.

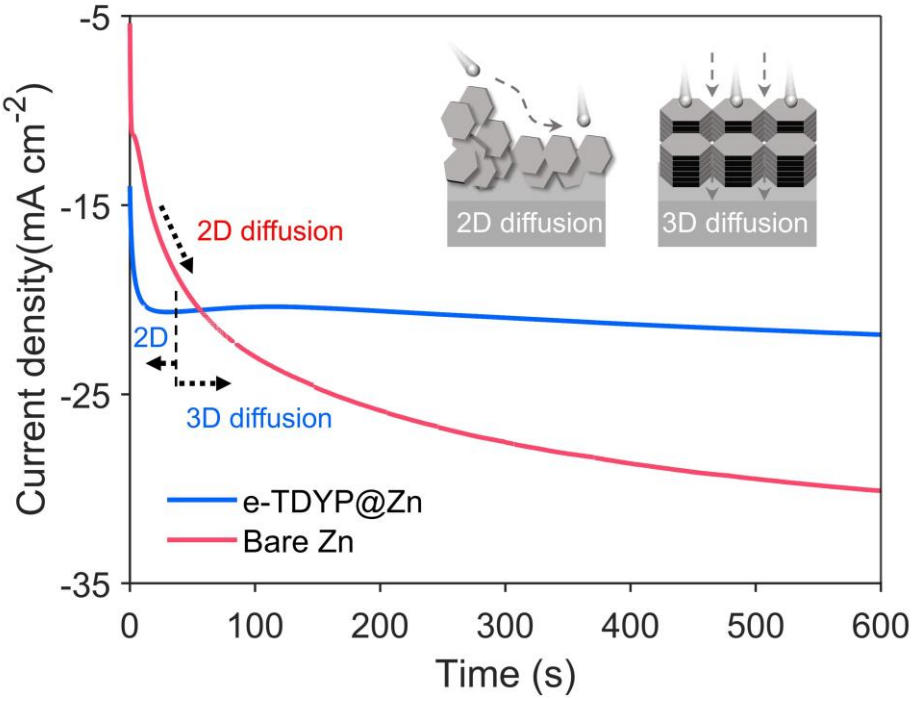

Fig. S16 Chronoamperometry (CA) test of e-TDYP@Zn and bare Zn electrodes.

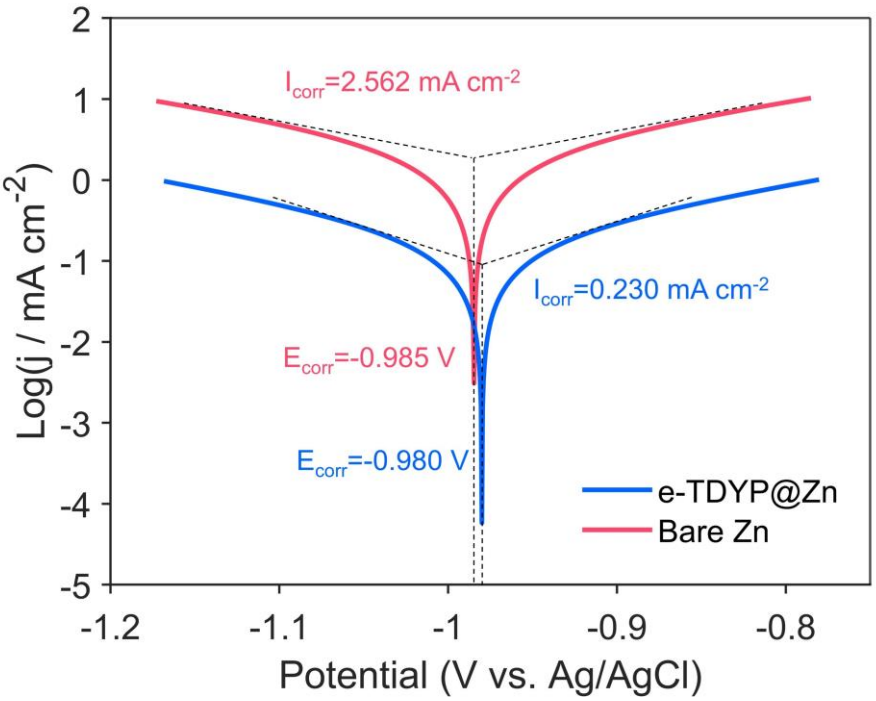

Fig. S17 Tafel curves and corresponding corrosion potential and current density.

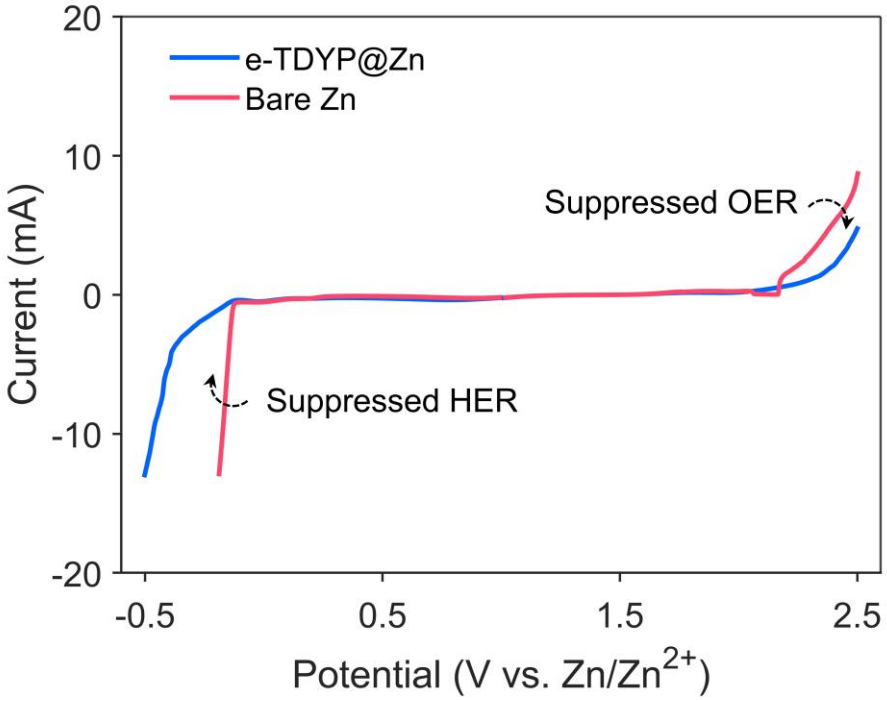

Fig. S18 LSV curves of e-TDYP@Zn and bare Zn at 1 mV s^{-1}.

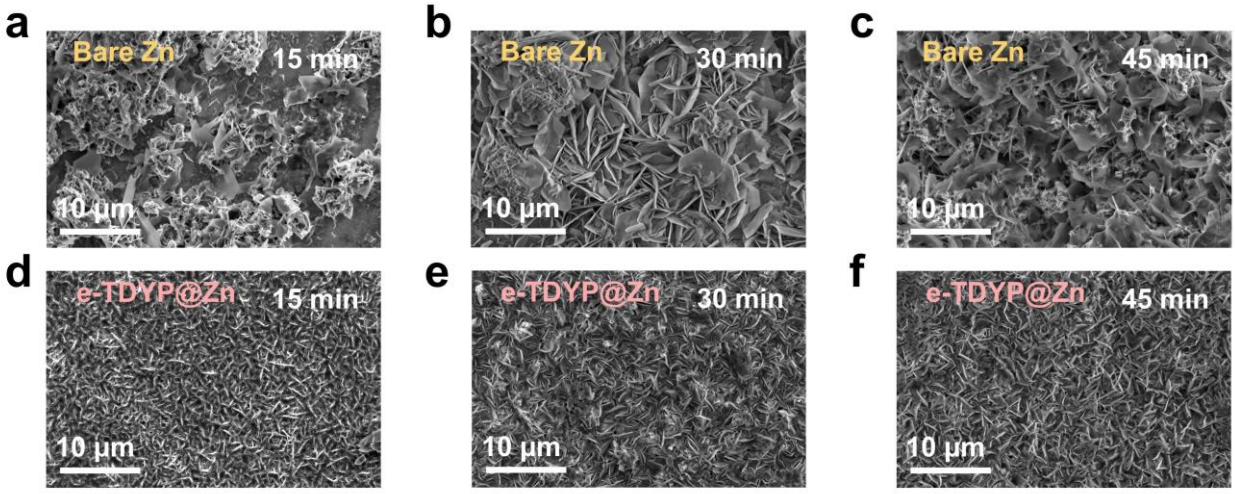

Fig. S19 SEM images of (a-c) bare Zn and (d-f) e-TDYP@Zn at different deposition time.

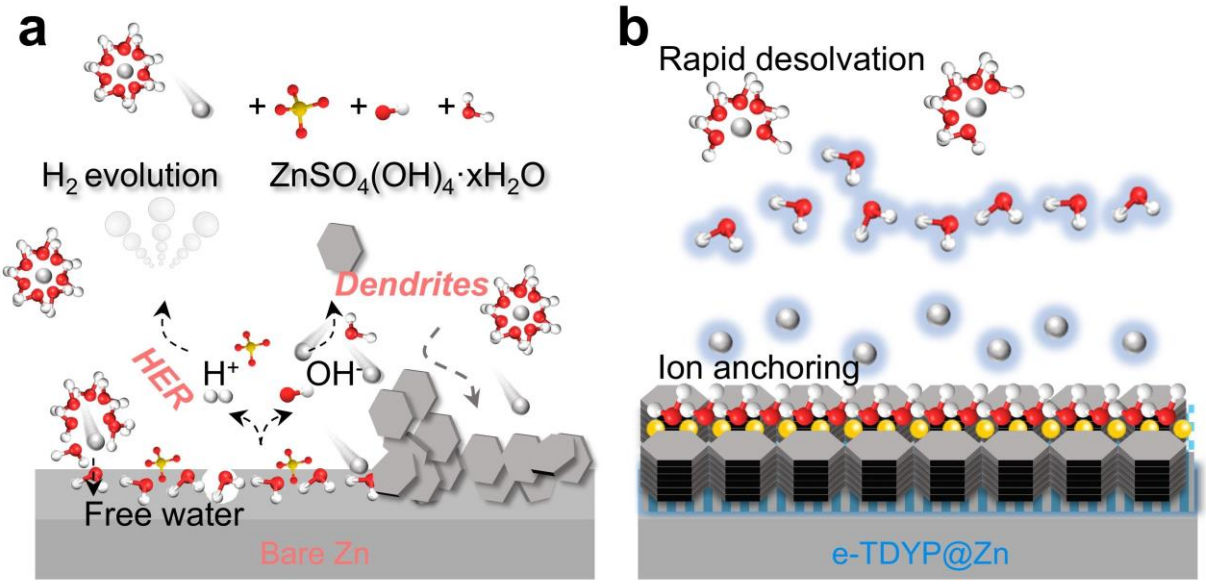

Fig. S20 Schematic illustration of the corrosion behavior of (a) bare Zn and (b) e-TDYP@Zn.

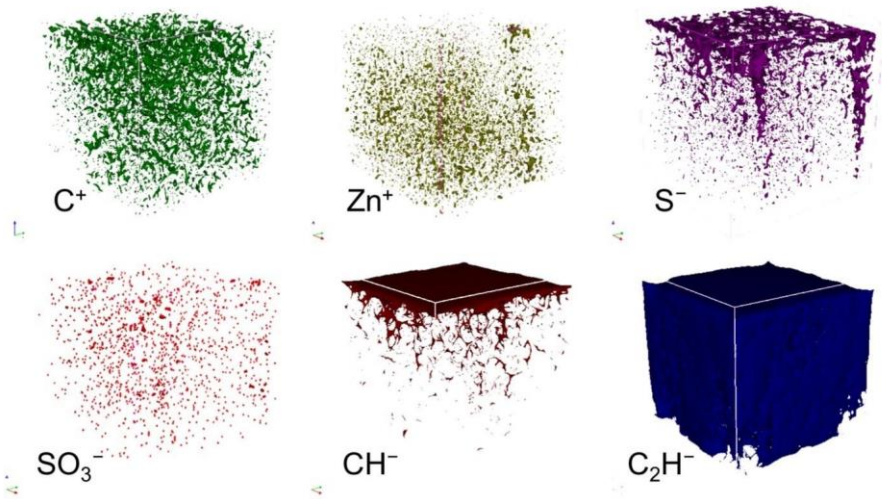

Fig. S21 Three-dimensional view of C^+, Zn^+, S^-, SO_3^-, CH^- and C_2H^- fragments distributions of e-TDYP@Zn in the TOF-SIMS sputtered volumes.

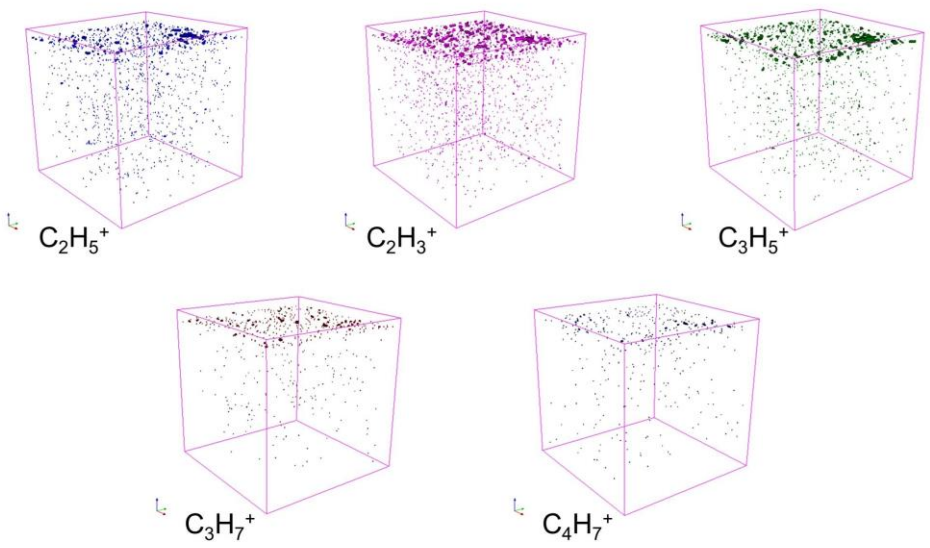

Fig. S22 Three-dimensional view of $C_2H_5^+$, $C_2H_3^+$, $C_3H_5^+$, $C_3H_7^+$, and $C_4H_7^+$ fragments distributions of e-TDYP@Zn in the TOF-SIMS sputtered volumes.

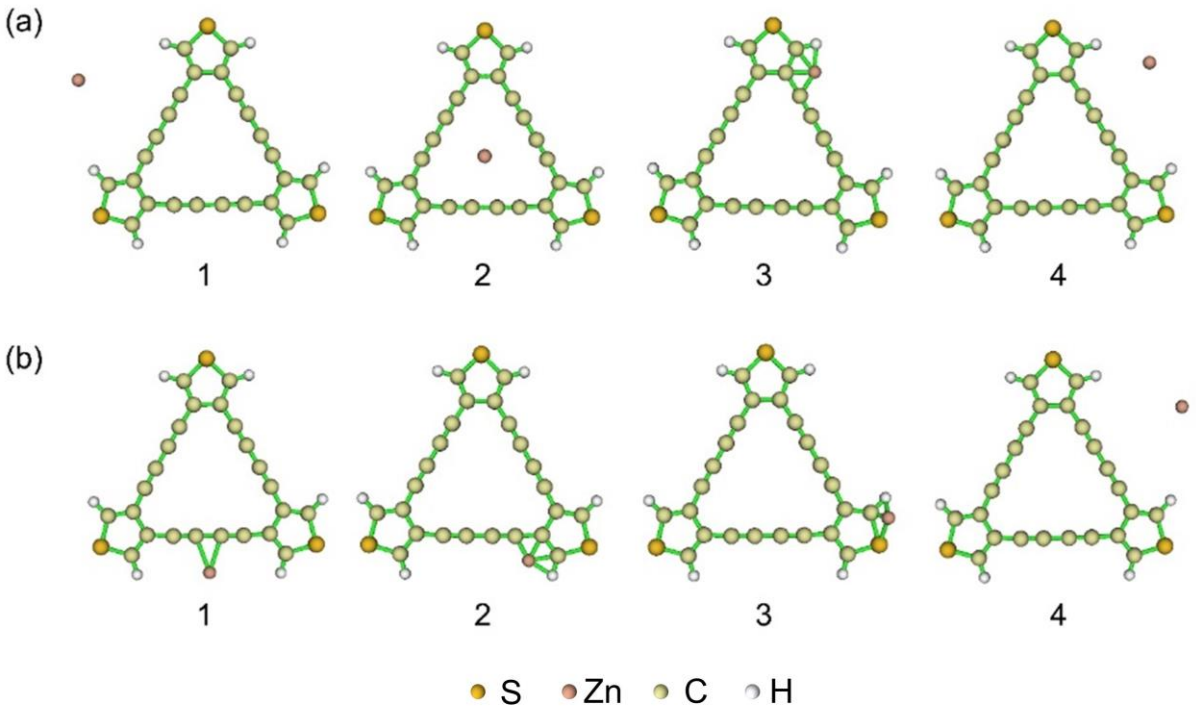

Fig. S23 Optimized structures of diffusion pathway of Zn^{2+} in the e-TDYP.

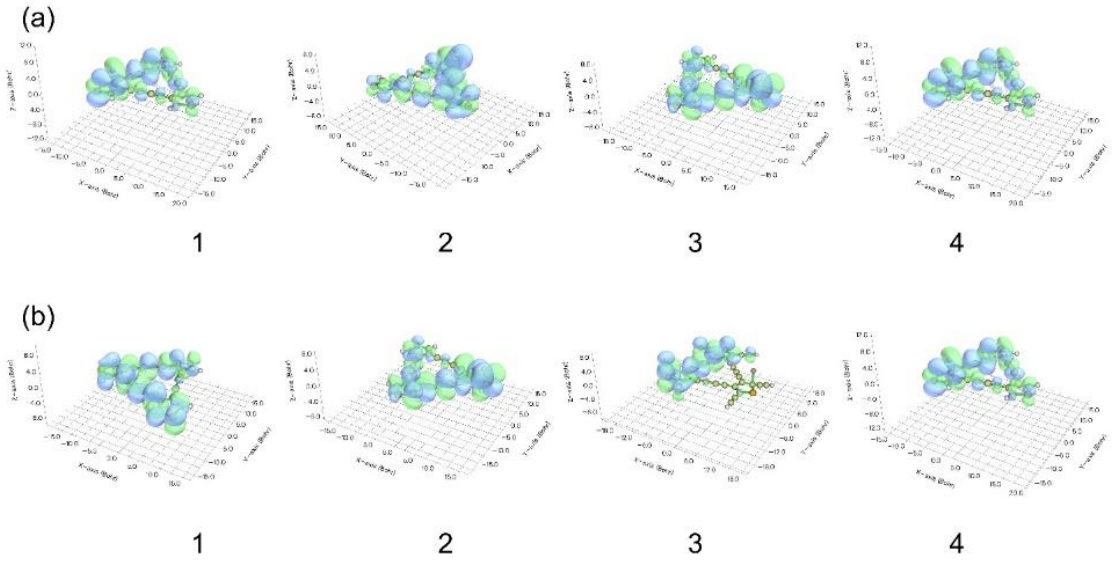

Fig. S24 Electron density distributions of Zn2+ in the e-TDYP.

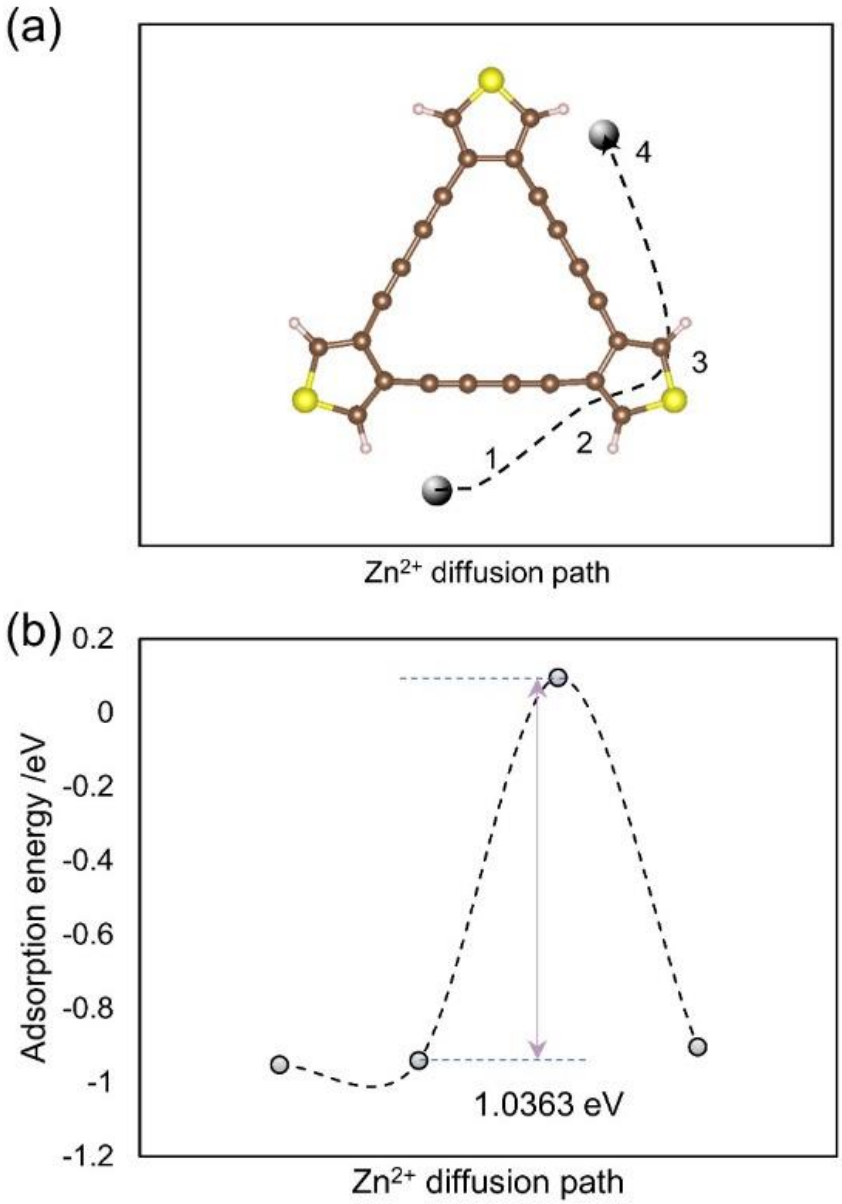

Fig. S25 (a) First-principles calculations of Zn^{2+} diffusion pathway in the e-TDYP bypassing the anchoring site of the cyclic diyne center and (b) the corresponding migration energy barrier.

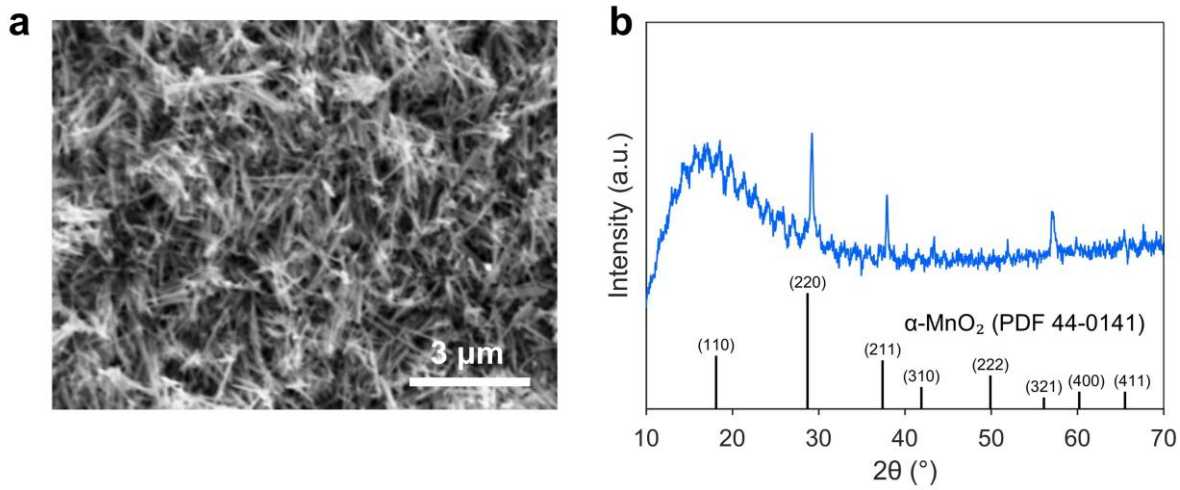

Fig. S26 (a) SEM image and (b) XRD pattern of the synthesized α-MnO_2.

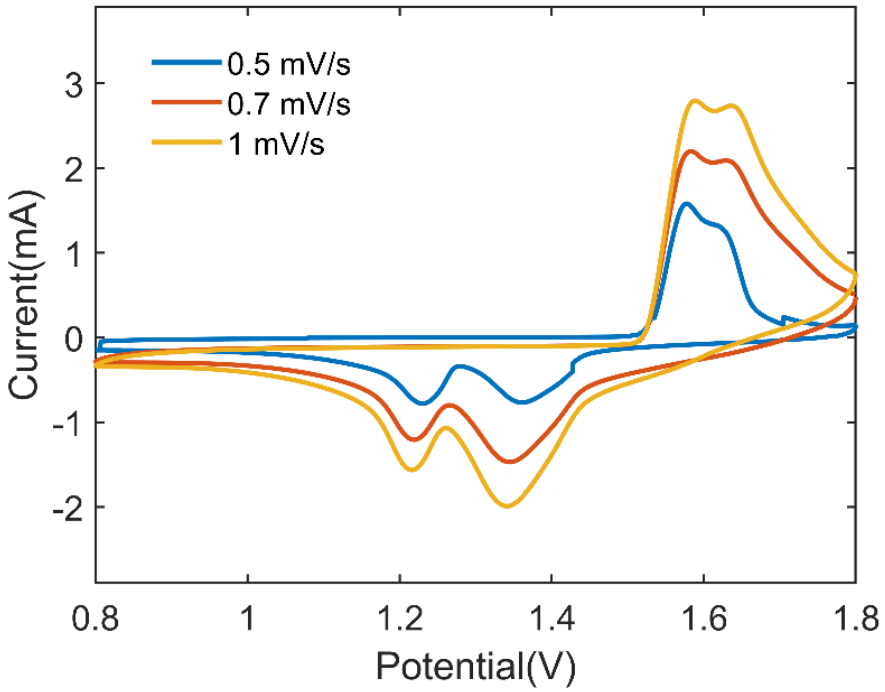

Fig. S27 CV curve of e-TDYP@Zn||MnO2 full cell under various scan rate.

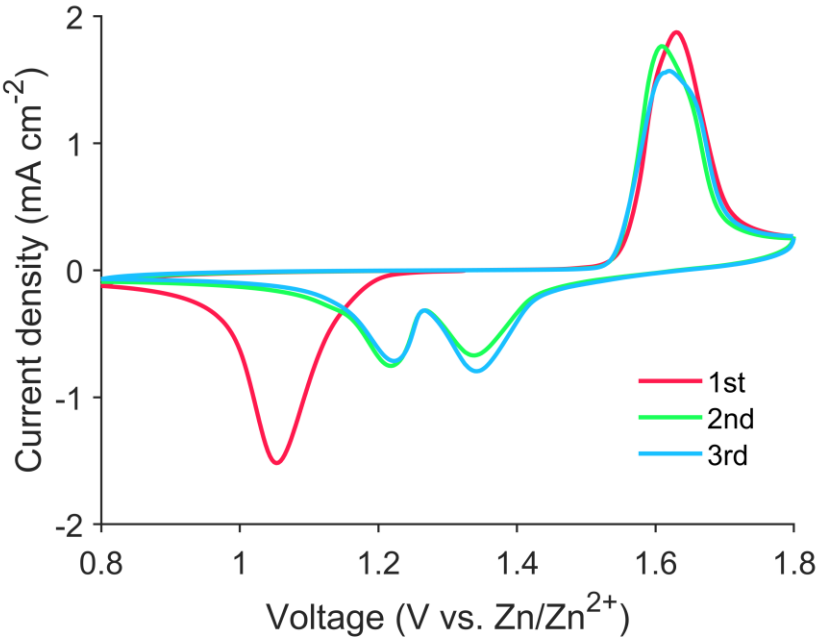

Fig. S28 CV curves recorded at the scan rate of 0.5 mV s^{-1} of bare Zn full cells.

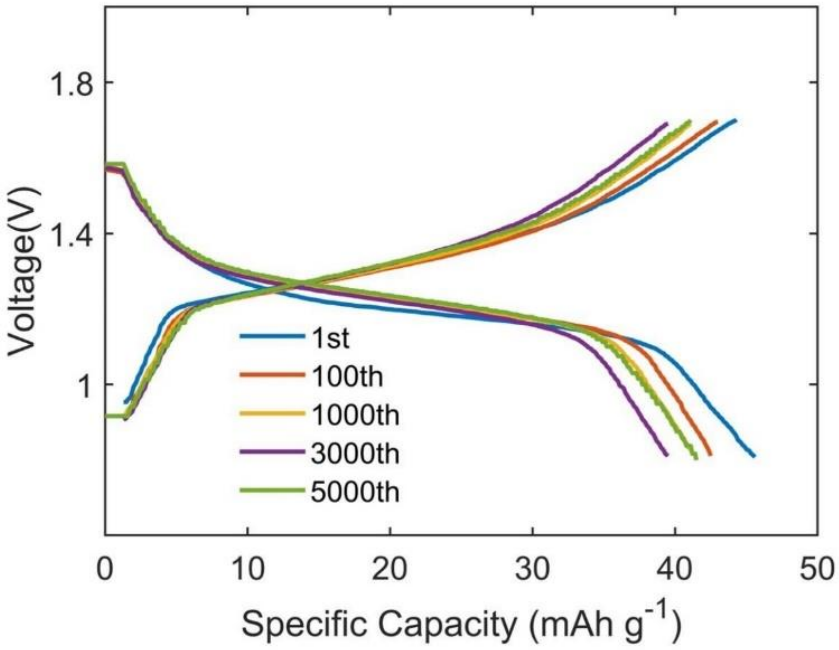

Fig. S29 Charge and discharge voltage profiles of e-TDYP@Zn||I_2 full cell at 1 A g^{-1}.

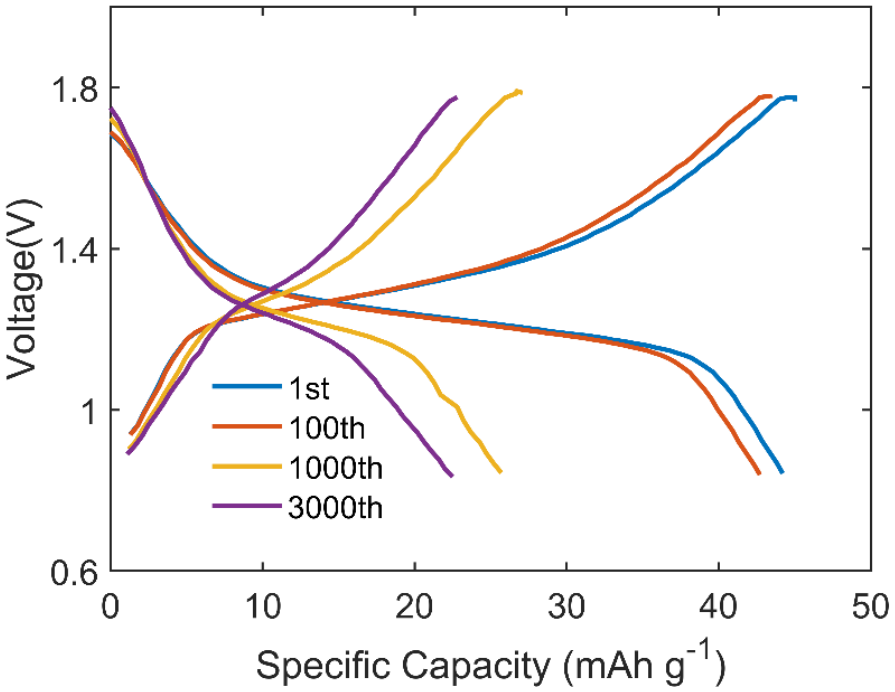

Fig. 30 Charge and discharge voltage profiles of Bare Zn||I_2 full cell at 1 A g^{-1}.

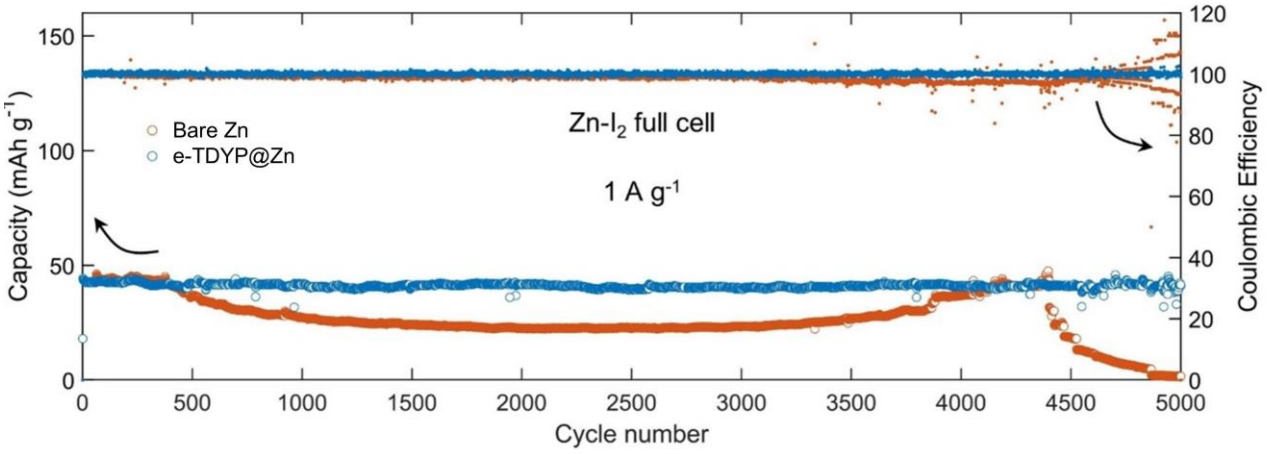

Fig. S31 Cycling performance of Zn||I_2 full cells at a current density of 1 A g^{-1}.

Tab. S1 | Long-term cycling performance comparison of e-TDYP@Zn symmetric cells with recent reports.

Symmetric cell	Current density (mA cm^{-2})	Areal capacity (mAh cm^{-2})	Lifespan (h)	Reference
e-TDYP@Zn	5	5	1200	This work
	10	10	250	
$(CS/SA)_4$–Zn	5	2.5	1750	*Adv. Mater.* 2024, **36**, 2306734
	10	10	210	
IM (002)Zn	5	5	1050	*Adv. Mater.* 2024, 2411004
	10	10	870	
ZSO/DN-0.09	5	5	550	*Angew. Chem. Int. Ed.*, 2024, **136**, e202403050
	8	8	130	
CIL@Zn	5	2	700	*Adv. Funct. Mater.* 2024, **34**, 2312855
	10	4	200	
Fs-Zn	10	1	1720	*Angew. Chem. Int. Ed.*, 2024, **136**, e202406292
	10	5	330	
P2VP-Zn	5	5	300	*Adv. Mater.* 2024, **36**, 2307727
Sn-Mxene-Zn	5	5	920	*Adv. Energy Mater.* 2024, **14**, 2400613
(002) etched-Zn	1	1	1650	*Energy Environ. Sci.*, 2024, **17**, 642-654
	10	5	500	